

Automatic DEM data classification of Mars lineament structure

Ziyi Li^a, Pengcheng Yan^b, Jiarui Liang^a and Xiaolin Tian^{*a,b}

^aFaculty of Information Technology, Macau University of Science and Technology, Macau, China;

^bLunar and Planetary Science Laboratory/Space Science Institute, Macau University of Science and Technology, Macau, China

ABSTRACT

This paper presents an automatic classification algorithm of Mars surface lineament structure based on Resnet50 in DEM (Digital Elevation Model) data. This work aims to reduce the time spent by planetary researchers on the collection of lineament structure samples, so as to concentrate on scientific research based on lineament structure data. This method avoids the problems that traditional DTA (Digital Terrain Analysis) technology can only be used locally and the judgment threshold is difficult to set due to the large differences in Mars around the planet. The highest accuracy of crater is 98.15%, the highest accuracy of dorsum is 100%, the highest accuracy of Vallis is 94.44%, and the highest total accuracy is 87.96%.

Keywords: DEM data, Mars surface, lineament structure, Resnet

1. INTRODUCTION

1.1 Background and motivation

There are various landforms on Mars, and the lineament structure is a very significant landform¹⁻³. We need a deeper study of these landforms to further the exploration of the reasons for their formation and restore the process of landform changes on Mars⁴. And a large volume of samples is the indispensable foundation of the more in-depth research.

Unlike CCD (Charge Coupled Device) images, the gray level of DEM images does not express light intensity information, but altitude information. Therefore, the DEM image can more directly reflect the difference between the two lineament structures (Dorsum and Vallis). With the development of deep space exploration, more and more high-quality image sources have appeared, waiting to be classified to produce sample sets to facilitate subsequent research. The resolution of the currently published DEM images after processing can already identify most of the named landforms.

Traditionally, it is necessary to manually classify samples of various landforms on the surface of Mars, which will cost a lot of labour and time. At present, there have been many applications of convolutional networks to image classification. This article will try to use Resnet50 to automatically classify the lineament structure of the global surface of Mars.

1.2 Related works

In processing the terrain automatic classification of DEM image samples, most of them are still using DTA technology, using terrain feature factors (slope, profile/vertical curvature etc.)⁵. However, due to the large differences in texture, size, shape, position and layout of the various elements on the surface of Mars. There is a big difference between the northern and southern hemispheres of Mars⁶. Under this method, it is more difficult to set the judgment threshold, and most of them can only automatically classify a certain area of Mars⁷⁻¹⁰.

2. DATA SET

2.1 DEM image source (USGS Astrogeology Science Center)

Mars MGS MOLA-MEX HRSC Hybrid DEM Global 200m v2 be used in this article. The resolution for this DEM data is 200 meters per pixel (m).

*xltian@must.edu.mo

2.2 Original samples

The samples are divided into three types (Dorsum, Vallis, Crater, as shown in Figures 1-3) 300 samples of each type, a total of 900 samples.

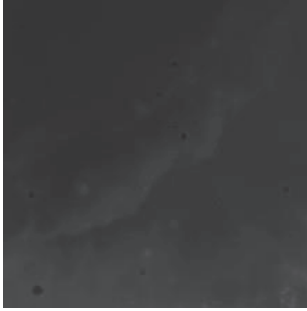


Figure 1. A Dorsum.

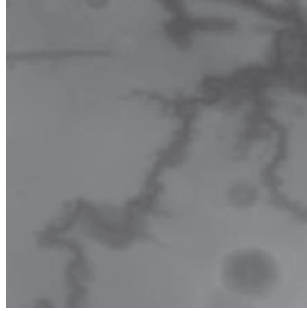


Figure 2. A Vallis.

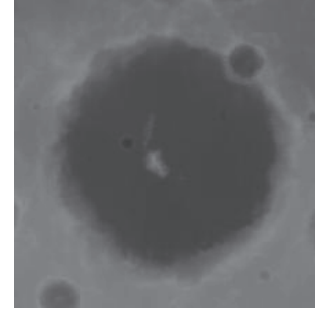


Figure 3. A Crater.

In the 34 named Dorsum of Mars. Dorsum that are too small or at high latitudes are eliminated. Because DEM images do not have the same high resolution as CCD images, some Dorsum that are too small are difficult to use as samples and some Dorsum at high latitudes have image distortion. Then 13 Dorsum are selected to make 60 original samples. Among them, 31 original samples (51.67%) were difficult to see with the naked eye before pre-treatments, as shown in Figure 4.

There are 156 named Vallis. Based on the same principle, 25 of them are selected and 60 original samples are intercepted. Among them, 24 original samples (40.00%) were difficult to see with the naked eye before pre-treatments, as shown in Figure 5.

The crater was added as the non-linear structures. Mars has 1138 named Craters. Based on the same principle, 60 Crater is selected and 60 original samples are intercepted. Among them, 4 original samples (6.67%) were difficult to see with the naked eye before pre-treatments, as shown in Figure 6.



Figure 4. A Dorsum was difficult to see.

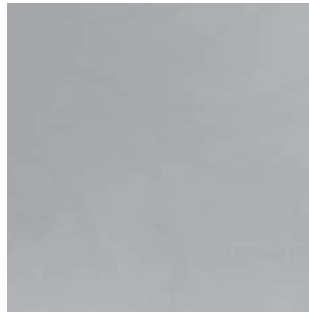


Figure 5. A Vallis was difficult to see.



Figure 6. A Crater was difficult to see.

2.3 Samples expansion

There are two sample sets of 300×3 and 540×3 samples respectively. Each original sample is 3D transformed to obtain 4 samples with x-axis rotation of $\pm 15^\circ$ and y-axis rotation of $\pm 15^\circ$, expanding each category from 60 to 300. Then on the basis of 300 samples, 240 samples rotated by $\pm 30^\circ$ were added to the 540 samples set.

2.4 Samples division

According to the ratio of 6:2:2, samples are completely randomly divided into train set, test set, and valid set. Of course, the original sample and its variants did not divide into different sets.

3. NETWORK

3.1 Resnet50

Resnet has a breakthrough over the previous network, which is the residual data unit (as shown in Figure 7). This structure solved the degradation problem and accelerated training. Then the network can be deeper and get better accuracy¹¹⁻¹².

3.2 Parameter setting

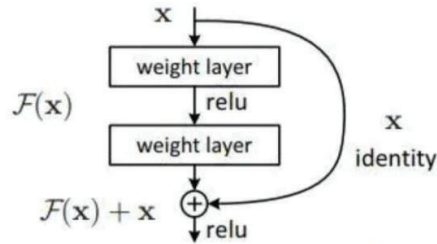


Figure 7. Residual block unit.

Set the learning rate to 1×10^{-5} , the weight decay to 5×10^{-4} , and the batch size to 30 for train set and 15 for test set. And the gradient algorithm selected SGD. In the automatic classification of CCD images of the lineament structure of Mars, 1200 epochs can see the accuracy convergence, and the accuracy of selecting pre-bottleneck will be higher than bottleneck, so select 1200 epoch and pre-bottleneck.

3.3 Accuracy

The accuracy calculation equation is shown in equation (1). And the average of the accuracy of the three categories is used as the total accuracy.

$$Acc_{Label} = \frac{Num_{Predicted}}{Num_{Correct}} \tag{1}$$

4. RESULTS AND ANALYSIS

Test Set Results: Through 1200 epochs to get the accuracy curve and loss curve, as shown in Figures 8-9 and Table 1.

Table 1. The accuracy of test set (540 samples).

Types	The highest accuracy	Average	Variance
Crater	98.15%	77.73%	72.69
Dorsum	100.00%	84.74%	285.90
Vallis	94.44%	69.53%	48.96
Total	87.96%	77.33%	35.80

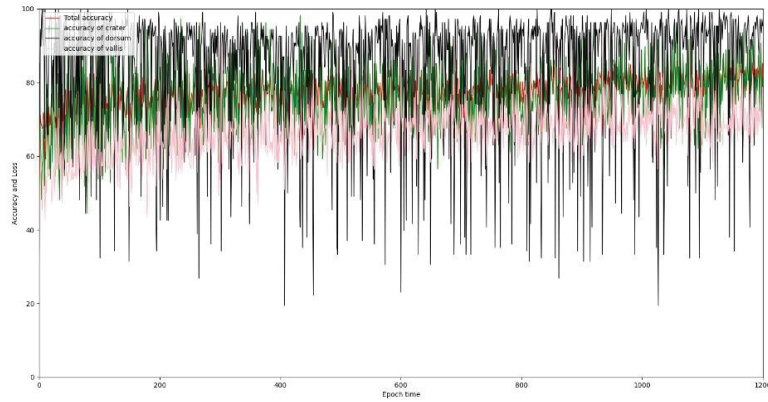


Figure 8. Accuracy after 1200 Epochs with test set (540 samples).

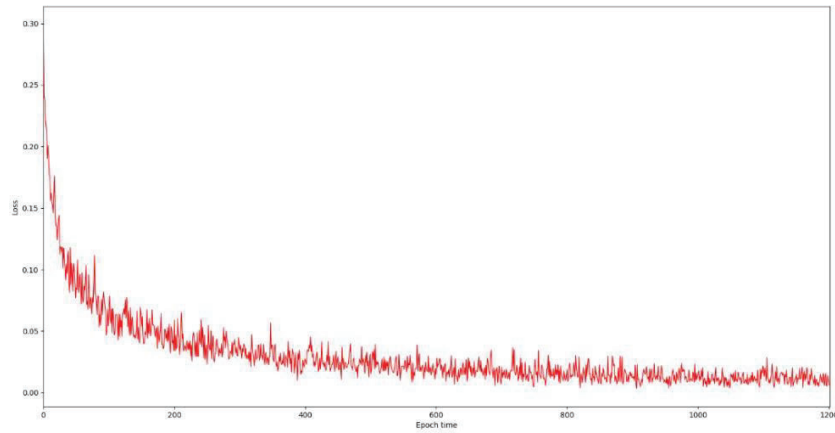


Figure 9. Loss after 1200 Epochs with test set (540 samples).

Valid Set Results: Through 1200 epochs to get the accuracy curve and loss curve, as shown in Figures 10-11 and Table 2.

Results Analysis: Compared with 300 samples, the 3D-transformation is used to further expand the number of samples to 540, which does not improve the accuracy, nor can it reduce the fluctuation of the accuracy. Contrasting the loss curves of the test set and the valid set, there is no overfitting.

Table 2. The accuracy of valid set (540 samples).

Types	The highest accuracy	Average	Variance
Crater	100.00%	97.63%	10.29
Dorsum	100.00%	88.49%	136.17
Vallis	100.00%	90.00%	30.12
Total	98.77%	92.04%	26.72

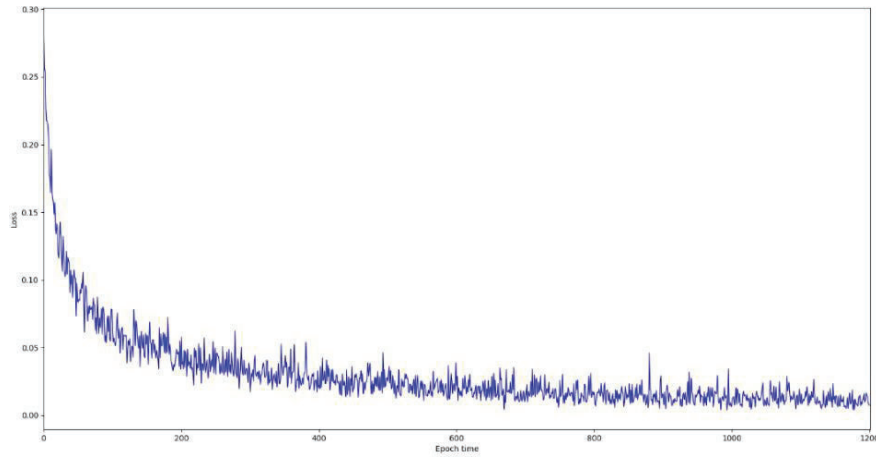


Figure 10. Accuracy after 1200 Epochs with valid set (540 samples).

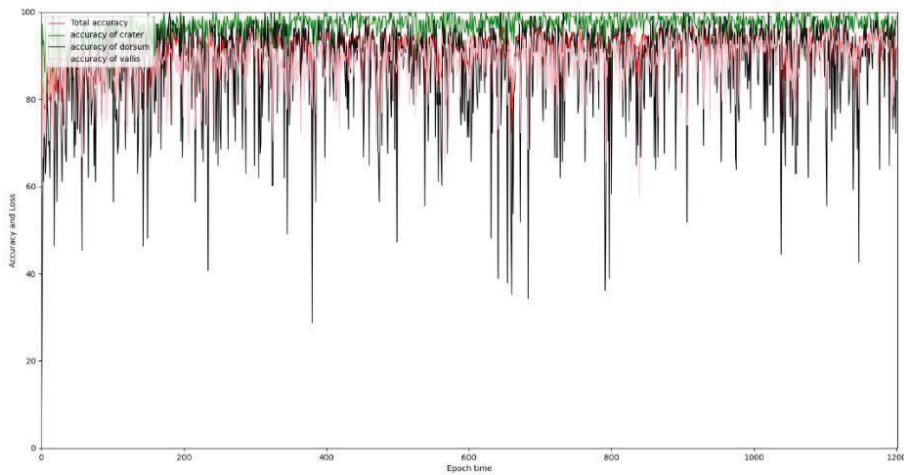


Figure 11. Loss after 1200 Epochs with valid set (540 samples).

5. CONCLUSION

Resnet50 performs very well in the automatic classification of the lineament structure of the Mars surface based on DEM images. The highest accuracy of crater is 98.15%, the highest accuracy of dorsum is 100%, the highest accuracy of Vallis is 94.44%, and the highest total accuracy is 87.96%.

Using 3D transformation to continue to expand the number of samples does not have a significant impact on the accuracy.

The follow-up work will deal with the problem of low resolution and low contrast of some DEM samples, carry out sample pre-processing, and research the influence of pre-processing on accuracy.

ACKNOWLEDGEMENT

This work is funded by The Science and Technology Development Fund, Macau SAR (File no. 039/2020/A1).

REFERENCES

- [1] Yan, P. C., Su, Y. and Tian, X., "Classification of mars lineament and non-lineament structure based on ResNet50," 2020 IEEE Inter. Conf. on Advances in Electrical Engineering and Computer Applications (AEECA) (IEEE).
- [2] Luo, L., Liu, J. Z., Zhang, L., Ji, J. Z., Guo, D. J. and Liu, J. W., "Research on the classification system of lunar lineaments," *Acta Petrologica Sinica*, 33(10), 3285-3301 (2017). (in Chinese with English abstract)
- [3] Komatsu, G. and Baker, V., "Formation of valleys and cataclysmic flood channels on Earth and Mars," *The Geology of Mars: Evidence from Earth-Based Analog*, 297-321 (2007).
- [4] Zhang, T. and Jin, S., [Automatic Recognition of Impact Craters on the Martian Surface from DEM and Images], Springer, Berlin Heidelberg, (2015).
- [5] Bue, B. and Stepinski, T. F., "Automated classification of landforms in Terra Cimmeria," 36th Annual Lunar and Planetary Science Conf., (2005).
- [6] Smith, D. E., "Erratum: The global topography of Mars and implications for surface evolution," *Science*, 1495-1502 (1999).
- [7] Wang, C., Hu, P., Liu, X H., et al., "Automated classification of martian landforms based on digital terrain analysis (DTA) technology," *Geomatics and Information Science of Wuhan University*, 34(4), 483-487 (2009).
- [8] Vaucouleur, G. D., Blunck, J., Da Vies, M., et al., "The new Martian nomenclature of the international Astronomical Union," *Icarus*, 26(1), 85-98 (1975).
- [9] Bandeira, L., Saraiva, J. and Pina, P., "Development of a methodology for automated crater detection on planetary images," *Iberian Conf. on Pattern Recognition and Image Analysis*, (2007).
- [10] Pedrosa, M. M., de Azevedo, S. D., da Silva E. A. and Dias, M. A., "Improved automatic impact crater detection on Mars based on morphological image processing and template matching," *Geomatics Natural Hazards & Risk*, 1-14 (2017).
- [11] He, K., Zhang, X., Ren, S. and Sun, J., "Deep residual learning for image recognition," *Proc. of the IEEE Conf. on Computer Vision and Pattern Recognition*, 770-778 (2016).
- [12] Szegedy, C., Ioffe, S., Vanhoucke, V. and Alemi, A. A., "Inception-v4, inception-Resnet and the impact of residual connections on learning," *Thirty-first AAAI Conf. on Artificial Intelligence*, (2017).